Introduction to microfluidics

Jonathan Cottet and Philippe Renaud

Ecole Polytechnique Fédérale de Lausanne (EPFL), Lausanne, Switzerland

Nomenclature

CM	Clausius-Mossotti factor
DEP	Dielectrophoresis
EDL	Electrical double layer
EOF	Electro-osmotic flow
LOC	Lab-on-a-chip
MEMS	Microelectromechanical systems
nDEP	Negative dielectrophoresis
pDEP	Positive dielectrophoresis
Pe	Peclet number
Re	Reynolds number

List of symbols

Constants

Symbol	Name	Value	Units
e	Elementary charge	1.6×10^{-19}	C
g	Gravitational acceleration	9.81	m s^{-2}
j	Imaginary number	$\sqrt{-1}$	–
k_B	Boltzmann constant	1.38×10^{-23}	J K^{-1}
N_A	Avogadro number	6.022×10^{23}	mol^{-1}
ϵ_0	Vacuum permittivity	8.854×10^{-12}	F m^{-1}

Variables

Symbol	Name	Units
A	Cross-sectional area	m^2
a, b	Dimensions	m
C	Capacitance	F
$c_{0,i}$	Bulk concentration of the ion i	mol L^{-1}
C_i	Concentration of solute	mol m^{-3}
d	Thickness of dielectric layer	m
D	Diffusion coefficient	$\text{m}^2\,\text{s}^{-1}$
E	Electric field	V m^{-1}
f	Frequency	Hz
h	Height	m
I	Electric current	A
L	Length	m
L_D	Diffusion length	m

$\mathcal{P}$	Perimeter	m
p	Pressure	Pa
P_c	Capillary pressure	Pa
Q	Flow rate	$m^3\,s^{-1}$
R_h	Hydrodynamic resistance	$Pa\,s\,m^{-3}$
r_h	Hydrodynamic radius	m
R, r, r_{ext}	Radius	m
$Re\{z\}$	Real part of a complex number z	–
t	Time	s
T	Temperature	K
t_D	Diffusion time	s
v	Velocity	$m\,s^{-1}$
V	Voltage	V
w	Width	m
z_i	Valence of the ion	–
β	Widening angle	°
γ	Surface tension	$N\,m^{-1}$
γ	Shear rate	–
ϵ_m, ϵ_r	Relative permittivity	–
ζ	Zeta potential	V
η	Dynamic viscosity	Pa s
θ	Contact angle	°
Λ	Darcy friction factor	–
μ_i	Electrophoretic mobility	$m^2\,V^{-1}\,s^{-1}$
ν	Kinematic viscosity	$m^2\,s^{-1}$
ρ	Density	$kg\,m^{-3}$
$\dot{\gamma}$	Shear stress	$N\,m^{-2}$
σ_i	Electrical conductivity	$S\,m^{-1}$
ω	Angular frequency	$rad\,s^{-1}$

1 What is microfluidics? A brief definition and history

Nowadays the general tendency is to scale down the sample volume needed for all biosensing or chemical analyses as well as to increase throughput and reduce cost with the use of parallelization. Such developments were enabled by many fields such as molecular analysis, biodefence, molecular biology, and microelectronics [1]. With the advent of photolithography for microelectronics and later on, microelectromechanical systems (MEMS), the possibility to reduce the size of structures guiding liquids provided a way forward to successfully displace and analyze molecules as well as cells. Today, the original hope to reduce both the size of laboratories and the amount of the sample needed have been translated into reality with the "lab-on-a-chip" (LOC) devices were both the handling of fluids and analyses are performed directly on chip as presented in Chapter 4.

Microfluidics is defined as the "Handling of fluids in technical apparatus having internal dimensions in the range of micrometers up to a few millimeters" [2]. More generally, the term microfluidics is used if one of the dimensions of the microfluidic structure is smaller than 1 mm.

Microfluidics can be distinguished from "macrofluidics" by the fact that some effects visible at the microscale start to be predominant. Particularly, viscosity starts to play an important role and the so-called laminar flow regime, where adjacent layers of fluids experience little to no mixing, is a typical characteristic.

If one of the dimensions is below 1 μm, the term nanofluidics is normally used and corresponds to a world where discrete effects such as surface effects have an important impact on the behavior of fluids and suspended species.

The typical orders of magnitude of parameters in a microfluidic chip are:

- Channel width below 100 μm and height from 1 to 100 μm
- Flow rates from $nL\,s^{-1}$ to $\mu L\,s^{-1}$
- Flow velocity from $\mu m\,s^{-1}$ to $mm\,s^{-1}$ and $m\,s^{-1}$
- Volumes in the order of pL to μL.

Historically the first microfluidic devices were built in the 1940s for improving separation in electrophoresis when J. St. L Philpot proposed to combine laminar flow and an orthogonal electric field to separate proteins [3].

Since then, the field of microfluidics has considerably grown and its many advantages, as presented by Albert Folch [4], can be listed:

- Flow is often laminar and can be mathematically modeled.
- Microchannel sizes are of the same order of magnitude as biological cells, allowing direct interactions with cells for seeding and sorting as well as for probing a cell and its internal components.
- Automation can be provided on the system by microvalves and micropumps.
- Due to the small size of the fabricated devices, the batch production cost should be reduced.
- The amount of reagents used is smaller as well as the amount of sample needed.
- Analysis can be performed faster and in parallel.
- The compactness of the devices allows portability.
- The increase of the surface to volume ratio allows some processes such as thermal cycling to be accelerated.

Microfluidics is, therefore, a key technology for biotechnologies in fields ranging from health (personalized medicine, diagnosis) to biology (cell culture, bioprinting) as well as cosmetics (emulsions and formulations) and pharmaceuticals (drug discovery).

This chapter aims at offering the reader a broad presentation of the key concepts used in microfluidics to provide some guidance for understanding the forces and effects at play when designing microfluidic chips. Such understanding is critical for the comprehension of potential failure modes of microfluidics devices and troubleshooting, considerations that will be described in the following chapters.

1.1 Important mathematical background and notation

Throughout this chapter, a quantity in bold will correspond to a vectorial quantity (1).

$$v = \begin{pmatrix} v_x \\ v_y \\ v_z \end{pmatrix} \tag{1}$$

In the field of fluid mechanics and microfluidics, vectorial operators are often used. The operators Nabla ∇ and Laplacian Δ are defined as follows:

$$\nabla = \begin{pmatrix} \dfrac{\partial}{\partial x} \\ \dfrac{\partial}{\partial y} \\ \dfrac{\partial}{\partial z} \end{pmatrix} = \left(\dfrac{\partial}{\partial x}, \dfrac{\partial}{\partial y}, \dfrac{\partial}{\partial z} \right) \tag{2}$$

So:

$$\mathbf{grad}(p) = \nabla p = \begin{pmatrix} \dfrac{\partial p}{\partial x} \\ \dfrac{\partial p}{\partial y} \\ \dfrac{\partial p}{\partial z} \end{pmatrix} = \left(\dfrac{\partial p}{\partial x}, \dfrac{\partial p}{\partial y}, \dfrac{\partial p}{\partial z} \right) \tag{3}$$

$$div(v) = \nabla.v = \dfrac{\partial v_x}{\partial x} + \dfrac{\partial v_y}{\partial y} + \dfrac{\partial v_z}{\partial z} \tag{4}$$

$$\Delta p = \dfrac{\partial^2 p}{\partial x^2} + \dfrac{\partial^2 p}{\partial y^2} + \dfrac{\partial^2 p}{\partial z^2} \tag{5}$$

$$\Delta v = \begin{pmatrix} \dfrac{\partial^2 v_x}{\partial x^2} + \dfrac{\partial^2 v_x}{\partial y^2} + \dfrac{\partial^2 v_x}{\partial z^2} \\ \dfrac{\partial^2 v_y}{\partial x^2} + \dfrac{\partial^2 v_y}{\partial y^2} + \dfrac{\partial^2 v_y}{\partial z^2} \\ \dfrac{\partial^2 v_z}{\partial x^2} + \dfrac{\partial^2 v_z}{\partial y^2} + \dfrac{\partial^2 v_z}{\partial z^2} \end{pmatrix} \tag{6}$$

In particular, the gradient of a scalar quantity p is noted $\mathbf{grad}(p) = \nabla p$ and the divergence of a vectorial quantity $\mathbf{v}$ is div($\mathbf{v}$) = $\nabla . \mathbf{v}$.

Vectorial operators expressed in the different coordinate systems can be found elsewhere [5].

1.2 Fluid definition

A fluid is characterized by the property that it will deform continuously and with ease under the action of external forces [6]. Both liquids and gases can be considered as fluids and their shape will be determined by the container in which they are held. The field of study of fluid behavior is called fluid mechanics and is divided between fluid statics, where fluids are at rest, and fluid dynamics, where fluids are in motion. The following section is dedicated to the study of the equations governing fluids mechanics. In most cases, the fluid considered is Newtonian (its viscosity does not depend on the stress applied and is constant) and incompressible ($\mathrm{div}(\mathbf{v}) = 0$) as it is the case for aqueous solutions.

1.3 Navier-stokes equation

Applying Newton's second law of motion on a small element of a Newtonian incompressible fluid with constant viscosity, we obtain Eq. (7).

$$\rho \frac{dv}{dt} = \rho g - \nabla p + \eta \Delta v \qquad (7)$$

where **v** is the flow velocity (expressed in m s^{-1}), ρ is the density of the fluid (kg m^{-3}), t is the time (s), **g** is the gravitational acceleration ($g = 9.81$ m s^{-2}), p is the pressure (Pa), and η is the dynamic viscosity (Pa s).

The Navier-Stokes equation is composed of several terms:

- The left term corresponds to the variation of the speed of a particle moving in space. As the speed depends on time and position, $\mathbf{v} = \mathbf{v}(\mathbf{r}, t)$. This derivative can be rewritten as Eq. (8).

$$\frac{dv}{dt} = \frac{\partial v}{\partial t} + (v.\nabla)v \qquad (8)$$

The Navier-Stokes equation can be rewritten as Eq. (9).

$$\rho \frac{\partial v}{\partial t} + \rho(v.\nabla)v = \rho g - \nabla p + \eta \Delta v \qquad (9)$$

The right side of the equation corresponds to the different forces applied to the fluid particle where:

- ρg corresponds to the volumic forces, in this case, the impact of gravity on the fluid.
- $-\nabla p$ is a surface force and corresponds to the impact of pressure on the fluid.
- $\eta \Delta v$ is a volumic equivalent of the viscosity forces. The dynamic viscosity is usually expressed in poise (symbol P or Po) where 1 Po = 0.1 Pa s. At 20°C and constant atmospheric pressure, $\eta_{\mathrm{water}} = 0.01$ Po = 1 cPo and $\eta_{\mathrm{air}} = 0.018$ cPo.

1.4 Reynolds number

To characterize the fluid regime in fluidics, a dimensionless number is often used, the Reynolds number, abbreviated Re, and is defined as the ratio of inertial forces to viscous forces expressed in Eq. (10).

$$Re = \frac{\rho v L}{\eta} = \frac{v L}{\nu} \qquad (10)$$

where v is the typical velocity in the microchannel (m s^{-1}) and L is the characteristic dimension of the microchannel (m), for example, the diameter for a pipe. Additionally ν, the kinematic viscosity (expressed in m^2 s^{-1} or stokes (symbol St) where 1 $St = 1$ cm^2 s^{-1}), can be defined as (9)

$$\nu = \frac{\eta}{\rho} \qquad (11)$$

Three different regimes can be distinguished [7–9]:

- If $Re < 2300$, the flow is laminar.
- If $2300 < Re < 4000$, a nonfully developed turbulence occurs.
- If $Re > 4000$, the flow is fully turbulent.

In microfluidics, $Re < 2300$ and the flow is typically laminar. For example, if one considers a pipe of diameter 10 µm and a water flow of 10^{-3} m/s, the calculated $Re = 10^{-2} \ll 2300$.

1.5 Flow profile in a cylinder

For a low Reynolds number, the Navier-Stokes equation can be simplified as (12).

$$\rho \frac{\partial \boldsymbol{v}}{\partial t} = \rho \boldsymbol{g} - \boldsymbol{\nabla} p + \eta \boldsymbol{\Delta} \boldsymbol{v} \qquad (12)$$

If we consider a permanent flow of a viscous Newtonian and incompressible fluid between P_{in} and P_{out} with $\Delta P = P_{in} - P_{out}$ in a horizontal pipe of radius R and length L, as presented in Fig. 1, we obtain (13).

$$\eta \boldsymbol{\Delta} \boldsymbol{v} = \boldsymbol{\nabla} p \qquad (13)$$

Due to the symmetry of the system around the z-axis, it is interesting to consider the cylindrical coordinate system in this example for the velocity (14).

$$\boldsymbol{v} = \boldsymbol{v}(\boldsymbol{r}) = \boldsymbol{v}(r, \theta, z) \qquad (14)$$

For the same reason, v does not depend on θ and is invariant along the z-axis (15).

$$\boldsymbol{v} = \boldsymbol{v}(r) \qquad (15)$$

The pressure is also constant over a slice of the pipe (16).

$$\frac{\partial p}{\partial z} = Constant = \frac{P_{out} - P_{in}}{L} = -\frac{\Delta P}{L} \qquad (16)$$

Projecting the Navier-Stokes equation along the z-axis and expressing the Laplacian in the cylindrical coordinate system, we obtain (17).

$$\frac{1}{r} \frac{\partial}{\partial r} \left(r \frac{\partial v_z}{\partial r} \right) + \frac{1}{r^2} \frac{\partial^2 v_z}{\partial \theta^2} + \frac{\partial^2 v_z}{\partial z^2} = -\frac{1}{\eta} \frac{\Delta P}{L} \qquad (17)$$

Since v and consequently v_z only depend on r, we obtain (18).

$$\frac{1}{r} \frac{\partial}{\partial r} \left(r \frac{\partial v_z}{\partial r} \right) = -\frac{1}{\eta} \frac{\Delta P}{L} \qquad (18)$$

Integrating this equation, we obtain (19).

$$v_z(r) = -\frac{1}{4\eta} \frac{\Delta P}{L} r^2 + A \, ln(r) + B \qquad (19)$$

Since $v_z(r = 0)$ should be of a finite value and $v_z(r = R) = 0$ (no slip condition), we have (20).

$$A = 0 \text{ and } B = \frac{1}{4\eta} \frac{\Delta P}{L} R^2 \qquad (20)$$

Therefore (21).

$$v_z(r) = \frac{1}{4\eta} \frac{\Delta P}{L} \left(R^2 - r^2 \right) \qquad (21)$$

The result is characteristic of the parabolic flow profile in the laminar regime and is illustrated in Fig. 2.

The flow rate over a pipe section is called the Hagen-Poiseuille law and is defined as (22).

$$Q = \int_{r=0}^{r=R} \int_{\theta=0}^{\theta=2\pi} v_z(r) \, dr \, d\theta \qquad (22)$$
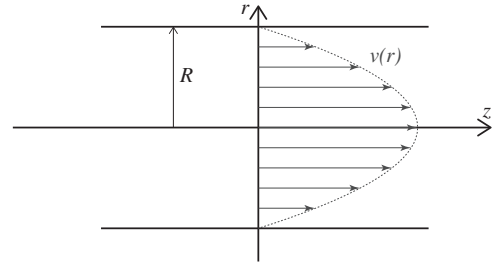

FIG. 1   Schematics of a cylinder of radius R and length L oriented along the z-axis with pressure P_{in} at the inlet and P_{out} at the oulet.

FIG. 2   Parabolic flow profile in a cylinder of diameter R.

$$Q = \int_{r=0}^{r=R} \frac{2\pi}{4\eta} \frac{\Delta P}{L} \left(R^2 - r^2\right) r \, dr$$

$$= \left[\frac{\pi}{2\eta} \frac{\Delta P}{L} \left(\frac{R^2 r^2}{2} - \frac{r^4}{4} \right) \right]_{r=0}^{r=R} \quad (23)$$

Therefore (24).

$$Q = \frac{\pi}{8\eta} \frac{\Delta P R^4}{L} \quad (24)$$

As presented in (24), the flow rate is proportional to R^4, hence reducing the diameter of a factor 2 will reduce the flow rate by a factor 16.

1.6 Analogy between electrical and hydraulic circuits

As demonstrated in the previous equation, the flow rate Q for a pipe is proportional to the pressure drop ΔP through a proportionality factor defined in (25) as the hydraulic resistance or hydrodynamic resistance R_h (in Pa s m^{-3} or kg m^{-4} s^{-1}).

$$R_h = \frac{\Delta P}{Q} = \frac{8\eta L}{\pi R^4} \quad (25)$$

This equation is completely analogous to Ohm's law and is often called the "fluidic Ohm's law." Indeed ΔP, the pressure drop, is similar to ΔV, the voltage drop along a wire, and Q, the flow rate, is similar to the electric current I through a wire and depends on the cross-section of the pipe. Table 1 presents values of hydrodynamic resistances for different classical cross-sectional shapes considering a straight channel of length L.

Hydrodynamic resistance formula is valid only after reaching the hydrodynamic entrance length, defined as "the duct length required to achieve a duct section maximum velocity of 99% of the corresponding fully developed magnitude when the entering flow is uniform" [10].

More formulas for different geometries can be found in [6] (parabola), [5] (eccentric annulus), [11] (triangular and trapezoidal cross-sections which are profiles often generated by microfabrication techniques), etc.

Thanks to this analogy, Kirchhoff laws can be applied in a microfluidic system and the following relationships can be written:

- For n resistances in series (26).

$$R_{h_{Total}} = \sum_{i=1}^{n} R_{h_i} \quad (26)$$

- For n resistances in parallel (27).

$$R_{h_{Total}} = \left(\sum_{i=1}^{n} \frac{1}{R_{h_i}} \right)^{-1} \quad (27)$$

1.7 Hydrostatic pressure

Hydrostatic pressure is the pressure present within a fluid in the absence of fluid motion. If the fluid is at rest, the Navier-Stokes equation can be simplified as the fundamental law of hydrostatics described in Eq. (28).
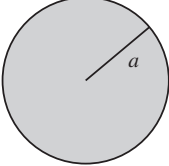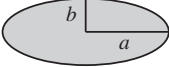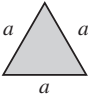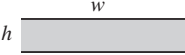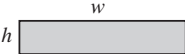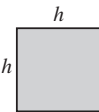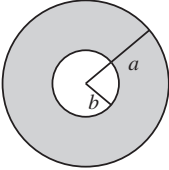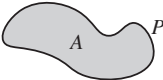
$$\rho g - \nabla p = 0 \quad (28)$$

This pressure should be considered for systems where a height difference between the reservoir and the microchannel exists.

1.8 Viscosity

"Viscosity is a quantitative measure of a fluid's resistance to flow. More specifically, it determines the fluid strain rate that is generated by a given applied shear stress" [12]. Microscopically it is linked to the cohesive forces between molecules and it is mostly affected by temperature and pressure. Those forces are normally larger between liquid molecules compared to gas molecules.

TABLE 1 Example of hydraulic resistances for different cross-sectional shapes of a straight channel The numerical values given for R_h are given considering $\eta = 1.\,10^{-3}$ Pa s, $L = 1$ mm, $a = 50$ μm, $b = 20$ μm, $h = 100$ μm and $w = 500$ μm. $\mathcal{P}$ is the perimeter and A the cross-sectional area

Shape	Figure	R_h Formula	R_h [10^{11} Pa s m^{-3}]
Circle		$\dfrac{8\eta L}{\pi a^4}$	4.07
Ellipse		$\dfrac{4}{\pi}\eta L\dfrac{1+\left(\dfrac{b}{a}\right)^2}{\left(\dfrac{b}{a}\right)^3}\dfrac{1}{a^4}$	36.92
Triangle		$\dfrac{320}{\sqrt{3}}\dfrac{\eta L}{a^4}$	295.6
Two plates		$12\dfrac{\eta L}{h^3 w}$	0.24
Rectangle		$\dfrac{12}{1-0.63\left(\dfrac{h}{w}\right)}\dfrac{\eta L}{h^3 w}$	0.27
Square		$28.4\dfrac{\eta L}{h^4}$	2.84
Concentric annulus		$\dfrac{8\eta L}{\pi}\dfrac{1}{\left(a^4-b^4-\dfrac{(a^2-b^2)^2}{\ln\left(\dfrac{a}{b}\right)}\right)}$	19.9
Arbitrary		$\approx 2\eta L\dfrac{\mathcal{P}^2}{A^3}$	–

Adapted from H. Bruus. Theoretical Microfluidics, OUP, Oxford, 2008; F.M. White. Viscous Fluid Flow, McGraw-Hill, New York, 2006.

1.9 Flow through porous media

Many applications in microfluidics require the fluid to go through different porous materials such as paper, membranes with nanopores, and gels. In this case, part of the fluid flows through the material while the rest of the fluid is trapped in pores. The law governing the flow

of a liquid in a porous material is known as Darcy's law [13] and is expressed in (29).

$$Q = \frac{\kappa A}{\eta L}\Delta P \qquad (29)$$

where Q is the flow rate (m^3 s^{-1}), κ is the permeability of the medium (m^2), A is the cross-sectional area of the flow (m^2), and η is the dynamic viscosity (Pa s).

1.10 Drag forces

For a particle immersed in a moving liquid, the fluid will exert a force, called hydrodynamic viscous drag force, on the nonmoving particle that will affect its velocity [14]. The fluid motion will cause this force to pull the particle along. If the particle is at the fluid velocity, no force is applied to the particle. As the flow in microsystems is usually laminar since the Reynolds number is small, this regime is called creeping flow or Stokes flow.

The expression of the drag force on a spherical particle, also known as Stokes law, is (30).

$$\boldsymbol{F_{Drag}} = 6\pi r_{ext}\eta \boldsymbol{v} \qquad (30)$$

where r_{ext} is the external radius of the particle, η is the dynamic viscosity of the medium, and v is the fluid velocity relative to the particle.

The constant term in front of **v** is called the friction factor and depends on the particle geometry [14, 15]. $6\pi r_{ext}\eta$ corresponds to the friction factor of a sphere. More coefficients for different geometries can be found in Ref. [15]. Such forces should be considered for liquid containing particles.

1.11 Diffusion

Diffusion is the macroscopic result of the random thermally driven motion of particles. It is described by Fick laws. Fick's first law of diffusion is expressed in Eq. (31).

$$J = -D\frac{\partial C_i}{\partial x} \qquad (31)$$

where C_i is the concentration of solute and D is the diffusivity also called the diffusion coefficient (in m^2 s^{-1} in SI units or cm^2 s^{-1} in CGS units) and is defined by the Stokes-Einstein relation (32).

$$D = \frac{k_B T}{6\pi\eta r_h} \qquad (32)$$

where $k_B = 1.380649 \times 10^{-23}$ J K^{-1} is the Boltzmann constant, T is the temperature (K), η is the dynamic viscosity, and r_h is the hydrodynamic radius of the particle (often approximated by the radius of the particle r_{ext}).

Fick's second law of diffusion (33) is related to the influence of diffusion on the change of concentration.

$$\frac{\partial C_i}{\partial t} = D\frac{\partial^2 C_i}{\partial x^2} \qquad (33)$$

The average diffusion length L_D in 1D is expressed in (34).

$$L_D = \sqrt{2Dt_D} \qquad (34)$$

where t_D is the diffusion time.

Another adimensional number comparing the different transport mechanisms is often used: the Peclet number, Pe, which can be defined as the rate of advection (transport by the fluid) to the rate of diffusion (35).

$$Pe = \frac{vL}{D} \qquad (35)$$

The higher the Peclet number, the more advection dominates over diffusion. For $Pe \gg 1$, convection dominates and large concentration gradients are possible whereas for $Pe \ll 1$, diffusion dominates and concentration is uniform in the volume.

1.12 Surface tension

Surface tension is "the property of the surface of a fluid that causes its surface to be attracted to another surface" [4, 16], expressed in $N\,m^{-1}$ in SI units. For liquids, surface tension is equivalent to the surface energy.

If we consider a drop of fluid or radius R immersed in another fluid and P_1 the pressure inside the drop and P_2 the pressure outside, we obtain the Young-Laplace equation (36).

$$P_1 - P_2 = \Delta P = \frac{\gamma}{R} \qquad (36)$$

where γ is the surface tension ($N\,m^{-1}$), R is the radius of the drop of fluid (m), and P is the pressure (Pa).

For a three-dimensional interface of arbitrary shape between two fluids, the Young-Laplace equation [17] becomes (37).

$$P = \gamma \left(\frac{1}{R_1} + \frac{1}{R_2} \right) \qquad (37)$$

where R_1 and R_2 are the two radii of principal curvature at the point considered and γ is the surface tension.

If we now consider a drop of liquid on a surface surrounded by gas as illustrated in Fig. 3, we obtain two possible cases depending on the value of the angle between the solid-liquid interface and the liquid-gas interface called "contact angle" θ:

- If $\theta > 90°$ and the liquid is water, the surface is said to be hydrophobic.
- If $\theta < 90°$ and the liquid is water, the surface is said to be hydrophilic.

For such a system, we can also write the law of Young-Dupré (38).

$$\gamma_{sg} - \gamma_{lg} \cos(\theta) - \gamma_{sl} = 0 \qquad (38)$$

where γ_{sl}, γ_{lg}, and γ_{sg} correspond, respectively, to the surface energy between solid-liquid, liquid-gas, and solid-gas.

It is important to notice that surface tensions are temperature sensitive and in most cases, the surface tension decreases with an increase in temperature.

1.13 Capillary action

Capillary action is the result of surface tension and corresponds to the ability of a liquid to flow spontaneously through thin pipes. If we consider a capillary filled with liquid as illustrated in Fig. 4, the capillary pressure obtain is presented in Eq. (39).

$$\Delta P_c = \frac{2\gamma \cos(\theta)}{R} \qquad (39)$$

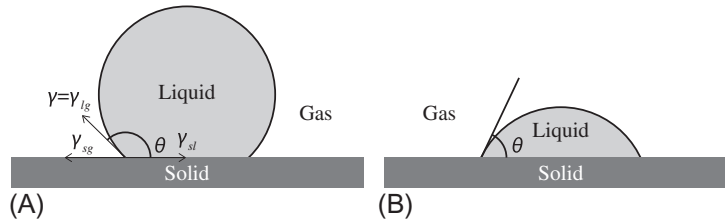where γ is the interfacial tension and R is the radius of curvature of the interface.

FIG. 3 Forces at the contact point. (A) Hydrophobic surface if $\theta > 90°$ and (B) Hydrophilic surface if $\theta < 90°$. γ_{sl}, γ_{lg}, and γ_{sg} correspond, respectively, to the surface energy between solid-liquid, liquid-gas, and solid-gas, respectively.
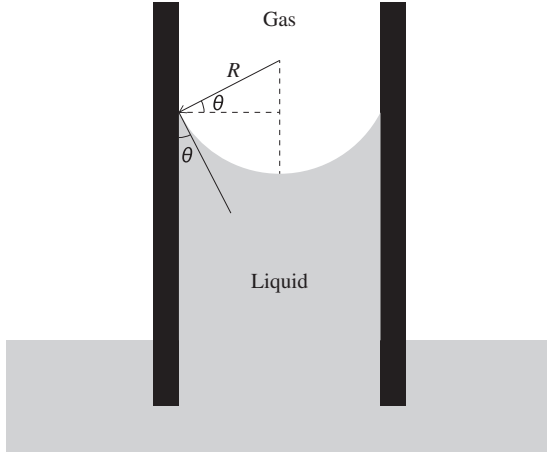
FIG. 4   Illustration of the capillary rise of a liquid in a hydrophilic capillary with R the radius of curvature of the interface and θ the contact angle.

For water at 20°C, in air, $\gamma = 7.28\ 10^{-2}\text{N m}^{-1}$. Assuming a 1 μm radius glass channel with $\theta = 45$ degrees, we obtain $\Delta P_c = 1$ bar.

If the contact angle is locally changed from $\theta_1 < 90$ degrees to $\theta_2 > 90$ degrees, the associated variation of capillary pressure is expressed in (40).

$$\Delta P_c = \frac{2\gamma_{gl}}{R}(cos(\theta_2) - cos(\theta_1)) < 0 \qquad (40)$$

The flow will stop at the beginning of the hydrophobic section: such an interface is also called a capillary stop. External pressure should be applied to overcome the pressure difference and restart the flow.

Similarly, if a rectangular channel of section w and height h locally widens with an angle β as presented in Fig. 5, the external pressure needed to overcome the pressure difference and restart the flow, also called burst pressure, is presented in Eq. (41) [18].

$$\Delta P_c = \frac{2\gamma}{w}\left(-\frac{w}{h}cos(\theta) - cos(\theta + \beta)\right) \qquad (41)$$

1.14 Head losses

For a real fluid, friction causes energy dissipation. This dissipation, called head loss, can be divided between "major losses" caused by energy dissipation per length of pipe and "minor losses" caused by changes of cross-section, bending, valves. They result in an equivalent loss of pressure in the pipe. For more details see Chapter 4 on LOC.

Major head losses are characterized by the Darcy-Weisbach equation (42).

$$\Delta P = \Lambda\frac{\rho v^2}{2} \qquad (42)$$

where Λ is the Darcy friction factor.

For short pipes, minor losses can exceed the major losses and can be estimated through tables.

1.15 Non-Newtonian fluids

Non-Newtonian fluids are fluids where the assumption of constant viscosity does not apply. Such cases can be modeled by Eq. (43).
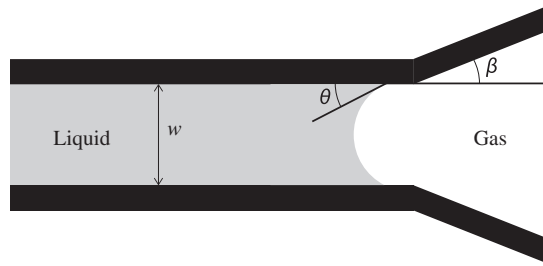

FIG. 5   Illustration of a capillary valve created by a widening of a rectangular microchannel of width w and height h.

$$\sigma = m\dot{\gamma}^n \qquad (43)$$

where σ is the shear stress and $\dot{\gamma}$ is the shear rate. The apparent viscosity can be expressed by the Ostwald-de Waele power-law model (44).

$$\eta = \frac{\sigma}{\dot{\gamma}} = m\dot{\gamma}^{n-1} \qquad (44)$$

The behavior of the fluid depends on the value of n, as illustrated in Fig. 6.

If $n < 1$, the fluid is non-Newtonian and displays a shear-thinning behavior also called pseudoplasticity. Examples of such fluids are polymer solutions or blood where the content (molecules or particles) is deformable and get stretched out with an increase in shear stress, resulting in the decreased viscosity.

If $n = 1$, the fluid is Newtonian and $\eta = m$.

If $n > 1$, the fluid is non-Newtonian with shear-thickening or dilatant behavior. Such behavior is displayed by some polymer solutions.

Typical values for different fluids can be found in Chhabra and Richarson [19].

2 Fluids in electrical fields

2.1 Electrophoresis

Electrophoresis corresponds to the movement of charged particles in a liquid under an applied electric field. It is often used to separate small ions and charged molecules (small and large such as DNA or proteins). Each charge is attracted by the electrode with the opposite charge. Because of friction forces, the maximum velocity v_i reached by an ion in an electrical field E is expressed in Eq. (45)

$$v_i = \frac{z_i e}{6\pi r_i \mu_i} E \qquad (45)$$

where z_i is the valence of the ion, e is the elementary charge ($e = 1.6 \times 10^{-19}$ C), r_i is the radius of the ion, and μ_i is the electrophoretic mobility.

The expression of the electrophoretic mobility for large molecules is given by Eq. (46).

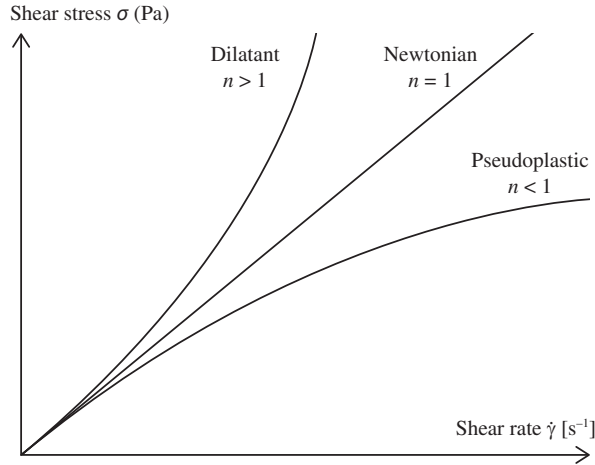$$\mu = \frac{v}{E} = \frac{\zeta D}{4\pi\eta} \qquad (46)$$

FIG. 6   Illustration of the evolution of the shear stress as a function of the shear rate for the different class of fluids: Dilatant ($n > 1$), Newtonian ($n = 1$) and Pseudoplastic ($n < 1$).

where ζ is the zeta potential and D the diffusion coefficient.

2.2 Electrical double layer

For a surface in contact with a solution, the charge of the surface will depend on the pH of the solution. For instance, for a glass surface composed of silanol groups (-Si-O-H) immersed in water with neutral pH, the hydroxyl groups will lose a proton and the surface will become negatively charged (-Si-O$^-$). The charge imbalance will be compensated by counter ions (also called counterions) from the solution, in the example positive ions, as presented in Fig. 7. This layer, also called the Debye layer or electrical double layer (EDL), is composed of two sublayers as described by Barz and Ehrhard [20]. The inner layer contains a fixed Stern layer and an almost immobile shear layer. The outer layer, called the diffusive layer, contains ions subjected to electrostatic interactions but still mobile. The zeta potential is defined as the potential at the interface between immobile and mobile layers corresponding to the shear plane. A more precise explanation taking into account the solvent molecules can be found in Pardon and van der Wijngaart [21].

The Debye length is the characteristic thickness of the Debye layer and corresponds to the distance over which the surface charges influence the distribution of charges in the solution. For a monovalent electrolyte, the Debye length is given by (47).

$$\lambda_D = \sqrt{\frac{\epsilon_m \epsilon_0 k_B T}{10^3 N_A e^2 \sum_i c_{0,i} z_i^2}} \tag{47}$$

where ϵ_m is the relative permittivity of the liquid, $\epsilon_0 = 8.854 \times 10^{-12}$ F m^{-1} is the vacuum permittivity, k_B is the Boltzmann constant, T is the temperature, $N_A = 6.022 \times 10^{23}$ J K^{-1} is the Avogadro number, e is the elementary charge, $c_{0,i}$ is the bulk concentration of the ion i (in mol L^{-1}), and z_i is the corresponding valence of this ion.

2.3 Electro-osmosis

If a pair of electrodes is used to apply an external electric field, the counterion layer is moved (toward the negative electrode for positive counterions for example). Because of the short distance between the molecules, the ions viscously drag the solution with them at the same speed. The flow profile, in this case, is flat and is commonly called the "plug flow profile" as presented in Fig. 8 (in opposition to the parabolic flow profile in pressure-driven flow presented in Fig. 2). This principle, called electro-osmotic flow (EOF), is commonly used in capillary electrophoresis systems.

It is important to notice that both electroosmosis and electrophoresis happen at the same time. EOF pumping is strongly dependent on the surface charges and is therefore influenced by adsorption and desorption. Typical devices using EOF pumping are presented in Chapter 3.
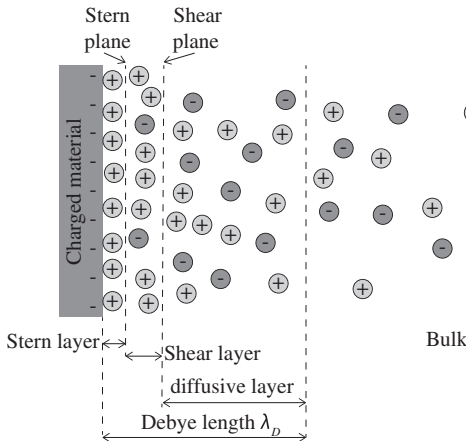

FIG. 7   Schematic of the double layer composed of an inner layer (Stern layer and shear layer) and the outer layer named diffusive layer. *Adapted from D.P. Barz, P. Ehrhard. Model and verification of electrokinetic flow and transport in a micro-electrophoresis device. Lab Chip 5(9) (2005) 949–958.*
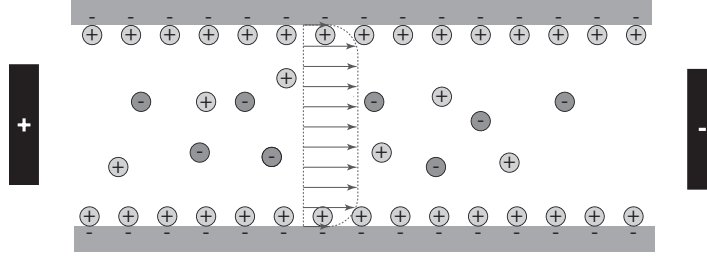
FIG. 8 Illustration of the electroosmotic flow in a microchannel between two electrodes located at each end. The flow is driven toward the negative electrode.
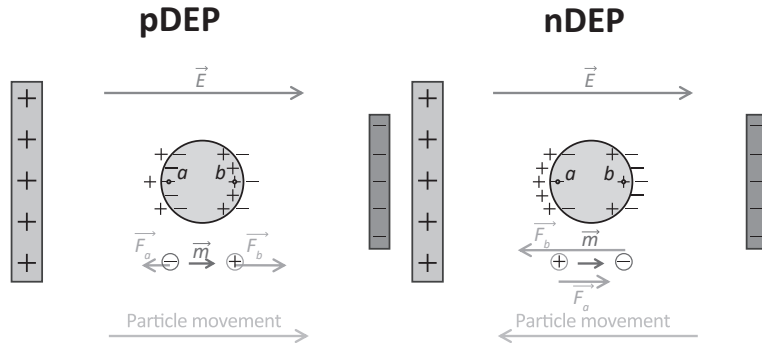

FIG. 9 Principle of (A) pDEP and (B) nDEP. E represents the electric field, m the dipolar moment, and F_a and F_b the Coulomb force ($F = qE$) on each barycenter of the charges on each side of the particle.

2.4 Dielectrophoresis

Dielectrophoresis (DEP) relies on the differences in dielectric properties between cells and their suspension liquid [22, 23]. Cells placed in a nonuniform electric field can, therefore, be either attracted in the high field region (positive dielectrophoresis or pDEP) or repelled in the low field region (negative dielectrophoresis or nDEP) as illustrated in Fig. 9.

The time average expression of the DEP force exerted on a polarizable particle (index p) of radius r_{ext} immersed in a suspending medium (index m) in a nonuniform electric field E is expressed in (48).

$$F_{DEP} = 2\pi\varepsilon_0\varepsilon_m r_{ext}^3 Re\{CM(f)\}\nabla E_{RMS}^2 \qquad (48)$$

where $CM(f)$ is the Clausius-Mossotti factor (49).

$$CM(f) = \frac{\varepsilon_p^* - \varepsilon_m^*}{\varepsilon_p^* + 2\varepsilon_m^*} \qquad (49)$$

and ε_i^* is the complex permittivity (50).

$$\varepsilon_i^* = \varepsilon_i\varepsilon_0 - \frac{j\sigma_i}{\omega} \qquad (50)$$

where ε_i is the relative permittivity, ε_0 is the vacuum permittivity, σ_i is the electrical conductivity (S m^{-1}), r_{ext} is the external radius of the particle, $\omega = 2\pi f$ is the angular frequency with f, the frequency of the electric field E. Tools are available for simulating the behavior of particles in a suspending medium [24].

DEP can, therefore, be used for various applications such as cell centering [26], cell separation [27], cell sorting [28], or cell aggregate creation [25].

2.5 Electrowetting

Electrowetting utilizes the electric field to modify the wettability of an electrolyte on a surface. It is defined as a "change in solid-electrolyte contact angle due to an applied potential difference between the solid and the electrolyte" [29].

If we consider a dielectric of thickness d and relative permittivity ε_r covering the electrode, the contact angle θ' is modified (51).

$$\gamma_{lg}\cos(\theta') = \gamma_{sg} - \gamma_{sl} + \frac{CV^2}{2} \qquad (51)$$

where $C = \frac{\varepsilon_r \varepsilon_0}{d}$ is the capacitance of the interface and V the applied voltage.

The principle is often used for electrowetting on dielectrics (abbreviated EWOD) where the base plate consists of an array of individually addressable electrodes, coated with a hydrophobic dielectric layer (e.g., Teflon thin film) and the top plate consists of a single ground electrode, coated with a hydrophobic dielectric layer. The space between the two plates is filled with an oil phase in which water droplets are inserted and manipulated. This concept is now known as digital microfluidics [30] and allows for the fluid motion to be completely automated but has some disadvantages such as the cost of the microfluidic chip.

3 Conclusion

Microfluidics is a relatively recent field that is concerned with the control of small amounts of liquids. As the channel dimensions decrease, effects, such as viscosity or surface tension, start to prevail. Fluid behavior becomes more predictable and, at low Reynolds numbers, the laminar flow regime dominates. Modifications in channel dimensions or surface properties can then be used to generate or stop the liquid flow. Furthermore, liquids as well as ions, molecules, and cells can be moved or separated by the use of an electric field.

Most of the phenomena that occur in microfluidics are described by the equations of fluid dynamics presented in this chapter. However, when at least one dimension is below 100 nm, discrete effects are predominant and define the world of nanofluidics. For example, if the Debye length—the thickness of the double layer—is similar or larger than the channel size, the flow will be mostly controlled by surface charges. Additionally, as channel size becomes even smaller, surface to volume effects start to be even more significant. Surfaces, indeed, play a major role in nanofluidics and surface energy is paramount. In channels below 50 nm, forces between atoms and molecules—called van der Waals forces—need to be considered. At this scale, for electroosmotic flows, the electrostatic forces between surface charges and a fluid containing charged particles will influence the flow dynamics. Additionally, density as well as charge distribution is not constant and is affected by intermolecular interactions. This field of nanofluidics is foreseen to open a new range of possibilities such as single-molecule analysis and manipulation, following rapid kinetics of chemical reactions.

References

[1] G.M. Whitesides, The origins and the future of microfluidics, Nature 442 (7101) (2006) 368–373.

[2] IWA23, Interoperability of Microfluidic Devices—Guidelines for Pitch Spacing Dimensions and Initial Device Classification, IWA 23:2016. I. T. T. M. B.-. groups 2016.

[3] J.S.L. Philpot, The use of thin layers in electrophoretic separation, Trans. Faraday Soc. 35 (3) (1940) 0038–0046.

[4] A. Folch, Introduction to bioMEMS, CRC Press, 2016.

[5] F.M. White, Viscous Fluid Flow, McGraw-Hill, New York, 2006.

[6] H. Bruus, Theoretical Microfluidics, OUP, Oxford, 2008.

[7] O. Reynolds, XXIX. An experimental investigation of the circumstances which determine whether the motion of water shall be direct or sinuous, and of the law of resistance in parallel channels, Philos. Trans. R. Soc. Lond. 174 (1883) 935–982.

[8] I. Wygnanski, M. Sokolov, D. Friedman, On transition in a pipe. Part 2. The equilibrium puff, J. Fluid Mech. 69 (2) (1975) 283–304.

[9] I.J. Wygnanski, F.H. Champagne, On transition in a pipe. Part 1. The origin of puffs and slugs and the flow in a turbulent slug, J. Fluid Mech. 59 (2) (1973) 281–335.

[10] R.K. Shah, A.L. London, Laminar Flow Forced Convection in Ducts, (1978) https://doi.org/10.1016/c2013-0-06152-x.

[11] D. Dumont-Fillon, D. Lamaison, E. Chappel, Design and characterization of 3-stack MEMS-based passive flow regulators for implantable and ambulatory infusion pumps, J. Microelectromech. Syst. (2020) 1–12.

[12] F.M. White, Fluid Mechanics, McGraw-Hill Education, 2016.

[13] S. Whitaker, Flow in porous media I: a theoretical derivation of Darcy's law, Transp. Porous Media 1 (1) (1986) 3–25.

[14] H. Morgan, N.G. Green, AC Electrokinetics: Colloids and Nanoparticles, Research Studies Press, Philadelphia, PA, 2003.

[15] H.C. Berg, N.J. Princeton (Ed.), Random Walks in Biology, Princeton University Press, 1993.

[16] P.-G. de Gennes, F. Brochard-Wyart, D. Quéré, Capillarity and Wetting Phenomena: Drops, Bubbles, Pearls, Waves, New York, Springer-Verlag, 2004.

[17] P. Tabeling, Introduction to Microfluidics, OUP, Oxford, 2005.

[18] J.M. Chen, P.-C. Huang, M.-G. Lin, Analysis and experiment of capillary valves for microfluidics on a rotating disk, Microfluid. Nanofluid. 4 (5) (2007) 427–437.

[19] R.P. Chhabra, J.F. Richarson, Non-Newtonian Flow and Applied Rheology, Butterworth-Heinemann, 2008.

[20] D.P. Barz, P. Ehrhard, Model and verification of electrokinetic flow and transport in a micro-electrophoresis device, Lab Chip 5 (9) (2005) 949–958.

[21] G. Pardon, W. van der Wijngaart, Modeling and simulation of electrostatically gated nanochannels, Adv. Colloid Interf. Sci. 199 (2013) 78–94.

[22] R. Pethig, Review article-dielectrophoresis: status of the theory, technology, and applications, Biomicrofluidics 4 (2) (2010) 022811.

[23] H.A. Pohl, The motion and precipitation of suspensoids in divergent electric fields, J. Appl. Phys. 22 (7) (1951) 869–871.

[24] J. Cottet, O. Fabregue, C. Berger, F. Buret, P. Renaud, M. Frénéa-Robin, MyDEP: a new computational tool for dielectric modeling of particles and cells, Biophys. J. 116 (1) (2019) 12–18.

[25] J. Cottet, A. Kehren, S. Lasli, H. van Lintel, F. Buret, M. Frénéa-Robin, P. Renaud, Dielectrophoresis-assisted creation of cell aggregates under flow conditions using planar electrodes, Electrophoresis 40 (10) (2019) 1498–1509.

[26] N. Demierre, T. Braschler, R. Muller, P. Renaud, Focusing and continuous separation of cells in a microfluidic device using lateral dielectrophoresis, Sens. Actuators B Chem. 132 (2) (2008) 388–396.

[27] P.R.C. Gascoyne, Y. Huang, R. Pethig, J. Vykoukal, F. F. Becker, Dielectrophoretic separation of mammalian-cells studied by computerized image-analysis, Meas. Sci. Technol. 3 (5) (1992) 439–445.

[28] S. Fiedler, S.G. Shirley, T. Schnelle, G. Fuhr, Dielectrophoretic sorting of particles and cells in a microsystem, Anal. Chem. 70 (9) (1998) 1909–1915.

[29] B.J. Kirby, Micro-and Nanoscale Fluid Mechanics: Transport in Microfluidic Devices, Cambridge University Press, 2010.

[30] H. Ren, R.B. Fair, M.G. Pollack, Automated on-chip droplet dispensing with volume control by electrowetting actuation and capacitance metering, Sens. Actuators B Chem. 98 (2–3) (2004) 319–327.

I. Microfluidics